Isothermal phase (vapour + liquid) equilibrium data for binary mixturesof propene (R1270) with either 1,1,2,3,3,3-hexafluoro-1-propene (R1216) or 2,2,3-trifluoro-3-(trifluoromethyl)oxirane in the temperature range of (279 to 318) K range.

Shalendra Clinton Subramoney, Wayne Michael Nelson, Xavier Courtial, Paramespri Naidoo, Christophe Coquelet, Dominique Richon, Deresh Ramjugernath

Isothermal vapor-liquid equilibrium data for binary mixtures of propene (R1270) with either 1,1,2,3,3,3-hexafluoro-1-propene (R1216) or 2,2,3-trifluoro-3-(trifluoromethyl)oxirane in the (279 to 318) K range.

Shalendra Clinton Subramoney[a], Wayne Michael Nelson[a,], Xavier Courtial[a], Paramespri Naidoo[a], Christophe Coquelet[a,b], Dominique Richon[a,c] and Deresh Ramjugernath[a,]*

[a]Thermodynamics Research Unit, School of Engineering, University of KwaZulu-Natal, Howard College Campus, Durban, South Africa

[b]MINES ParisTech, CTP - Centre Thermodynamique des Procédés, 35 Rue Saint Honoré, 77305 Fontainebleau Cedex, France

[c] FiDiPro, Department of Biotechnology and Chemical Technology, Aalto University, Kemistintie 1, PO Box 16100, Fi-00076 Aalto, Finland

*Corresponding author: E-mail: nelsonw@ukzn.ac.za; Tel.: +27 31 2603121; Fax: +27 31 2601118

Abstract

Isothermal vapor-liquid equilibrium data (*P*-*x*-*y*) are presented for the 1-propene +1,1,2,3,3,3-hexafluoroprop-1-ene and the 1-propene + 2,2,3-trifluoro-3-(trifluoromethyl)oxirane binary systems. Both binary systems were studied at five temperatures, ranging from (279.36 to 318.09) K, at pressures up to 2 MPa. The experimental vapor-liquid equilibrium data were measured using an apparatus based on the "static-analytic" method incorporating a single movable Rapid On-Line Sampler-Injector to sample the liquid and vapor phases at equilibrium. The expanded uncertainties are approximated on average as 0.07 K, 0.008 MPa, and 0.007 and 0.009 for the temperature, pressure, and both the liquid and vapor mole fractions, respectively. A homogenous maximum-pressure azeotrope was observed for both binary systems at all temperatures studied. The experimental data were correlated with the Peng-Robinson equation of state using the Mathias-Copeman alpha function, paired with the Wong-Sandler mixing rule and the Non-Random Two Liquid activity coefficient model. The model provided very satisfactory representation of the phase equilibrium data measured.

Keywords: VLE, hexafluoropropene, static-analytic, ROLSI^{TM}

1. Introduction

This study is part of an on-going research programme investigating the thermodynamic properties of fluorocarbons and their mixtures [1; 2; 3; 4; 5; 6], and more specifically isothermal phase behaviour for binary mixtures involving either 1,1,2,3,3,3-hexafluoroprop-1-ene or 2,2,3-trifluoro-3-(trifluoromethyl)oxirane [6; 7; 8; 9; 10; 11; 12]. Vapor-liquid equilibrium (VLE) data play an integral part in the design process of numerous unit operations and chemical processes. Furthermore, VLE data is a core necessity for the development and validation of correlative and predictive thermodynamic models. Accordingly, accurate VLE data are required for the calculation of interaction energies between functional groups for group contribution methods such as PSRK [13].

VLE data were measured for the binary systems of propene (R1270) + 1,1,2,3,3,3-hexafluoroprop-1-ene (R1216), and R1270 + trifluoro-3-(trifluoromethyl)oxirane. Trifluoro-3-(trifluoromethyl)oxirane is more commonly known as hexafluoropropylene oxide (HFPO). To the best of our knowledge no VLE data have been published for the R1270 + HFPO binary system, and thus, all data presented herein for this system are new data. Concerning the R1270 + R1216 binary system, isothermal VLE data have been measured by Coquelet *et al*. [6] in the temperature range from (263.17 to 353.14) K. The data corresponding to this work were measured within same temperature range but at different isothermal conditions. Consequently, they may considered as useful complementary data. These two binary systems exhibit homogenous pressure-maximum (positive) azeotropes within the investigated temperature range. The new experimental data were correlated with the Peng-Robinson (PR) [14] equation of state (EoS) integrating the Mathias-Copeman (MC) alpha function [15], the Wong-Sandler (WS) mixing rule [16] and the Non-Random Two Liquid (NRTL) activity coefficient model [17].

2. Experimental

2.1 Materials

Propene was supplied by Air Products (South Africa) with a certified purity greater than 0.9995 in volume fraction. 1,1,2,3,3,3-Hexafluoro-1-propene and 2,2,3-Trifluoro-3-(trifluoromethyl)oxirane were supplied by Pelchem (South Africa) with a certified purity greater than 0.999 in volume fraction. Apart from degassing via periodic vapor withdrawal, no further purification was undertaken. Gas chromatographic (GC) analysis is a classical method to validate the purities of each component. Unfortunately, all the impurities in each "pure" component are not known, and thus exact quantification was not possible. However, by GC analysis with a thermal conductivity detector (TCD) one can determine the ratio of peak areas of the impurities to the "pure" compound and thus give an indication of the purity of the sample. The Chemical Abstract Service (CAS) numbers, critical properties and molecular formulae of the relevant compounds are listed in table 1.

2.2 Apparatus

The apparatus used for the phase equilibrium measurements has been described in detail in previous works [10; 18], and thus, will only be discussed briefly herein. The apparatus follows the principle of the "static-analytic" method, and is conceptually similar to that of Laugier and Richon [19] and Valtz *et al.* [20]. The equilibrium cell (60 cm^3) is constructed of stainless steel 316 and is equipped with two sapphire sights. Isothermal conditions are attained by submerging the equilibrium cell into a thermo-regulated liquid solution. The temperature of this liquid solution is controlled via a immersion circulator (Grant; GR 150). The liquid phase within the equilibrium cell is agitated via a Teflon-coated magnetic stirrer bar driven by an external rotating magnet using a variable speed stirring device (Heidolph; RZR 2021).

The temperature within the equilibrium cell was measured by two 100 Ω platinum resistance thermometer (Pt100) probes inserted into cavities located at the top and base of the equilibrium cell respectively. The pressure within the equilibrium cell was measured via a 0 - 10 MPa gauge transmitter (WIKA; P-10). The pressure transmitter was housed within a thermo-regulated aluminium block, to ensure that fluctuations in the ambient temperature would not influence the output signal of the pressure transmitter. The line connecting the pressure transmitter to the equilibrium cell was heat-traced as it protrudes above the thermo-regulated liquid solution.

The signals from both the Pt100 probes and the pressure transmitter are recorded in real-time via a data acquisition unit (Agilent ; HP 34970A). Samples of both the liquid and vapor phases are withdrawn individually from the equilibrium cell via a single mobile Rapid On-Line Sampler-Injector (ROLSI^{TM}) [21]. The vaporized samples are transferred directly to the GC (Shimadzu; GC-17A) using a carrier gas (helium). The lines connecting the ROLSI^{TM} to the GC are heat-traced to ensure that the sample flushed to the GC remains homogenous. The GC is fitted with a stainless steel 316 packed column (Porapak Q, 3 m in length) and equipped with a TCD. Chromatograph peak analyses and integrations are performed using GC solutions V. 2.3 (Shimadzu).

2.3 Calibrations

The Pt100 probes were calibrated against a standard CTH 6500 calibration unit (WIKA). The P-10 pressure transmitter was calibrated against a CPH 6000 reference transmitter (WIKA). The reference instruments (CTH 6500 and CPH 6000) were calibrated by WIKA. The response of the TCD was calibrated by injecting known amounts of each component (direct injection method) via gastight syringes (SGE Analytic Science). The volumes of the gaseous components injected into the GC for calibration of the TCD ranged from 100 μL to 1 mL. The volume of injected gas was converted to the number of moles of component using the

ideal gas equation. The pressure and temperature of the injected gas were assumed to be equal to the ambient conditions.

2.4 Experimental procedure

The loading lines and equilibrium cell were evacuated and the heavier component (R1216 or HFPO) was introduced first. Then the lighter component, propene, was subsequently charged into the equilibrium cell corresponding to the desired pressure for the first measurement. The cell contents were agitated, to ensure attainment of equilibrium. The line connecting the pressure transmitter to the equilibrium cell was heated to a temperature ten degrees above the cell temperature. Phase equilibrium was assumed to have been reached when the pressure readings stabilized, i.e. the pressure was constant for a period of at least 10 minutes, within the uncertainty of measurement. At equilibrium, both the vapor and liquid phases were sampled individually using the ROLSI^{TM}. At least five samples for both the liquid and the vapor phases were analysed to check for measurement repeatability. Further equilibrium mixtures were prepared by adding additional amounts of propene; the abovementioned sampling procedure was repeated for each new mixture at equilibrium. The full procedure was repeated for the measurement of each *P-x-y* isotherm.

2.5 Experimental uncertainty

The estimation of experimental uncertainty has been detailed in communications by the National Institute of Standards and Technology (NIST) [22]. Furthermore, we have described in detail the procedures used to estimate the uncertainty with regard to VLE measurements in our previous work [12]. Briefly, the uncertainties are combined were necessary via *the law of propagation of errors*, which is based on a first-order Taylor series approximation [22]. The standard uncertainties for the variables in question are listed in table 2. The combined uncertainties $u(\theta_i)$ were converted to the combined expanded uncertainties $U(\theta_i)$ by applying a coverage factor of 2 (k = 2). The expanded uncertainty for temperature and

pressure are: $U(T)$ = 0.07 K and $U(P)$ = 0.008 MPa respectively. Regarding phase composition, the expanded uncertainty for the liquid and vapor phase compositions were estimated on average as: $U(x)$ = 0.007 and $U(y)$ = 0.009.

2.6 Data treatment

Modeling of the high-pressure VLE data was undertaken using in-house thermodynamic software developed at the Mines ParisTech CTP laboratory [23]. The experimental data were regressed using the symmetric phi-phi approach, by coupling the PR equation of state with the NRTL activity coefficient model and WS mixing rule. The representation of vapor pressures with the PR-EoS was improved using the MC alpha function. Regression of the VLE data involves the adjustment of three binary interaction parameters; two associated with the NRTL activity coefficient model (τ_{12}, τ_{21}), and one associated with the WS mixing rule (k_{12}). The NRTL parameters (τ_{12}, τ_{21}) are those originally proposed by Renon and Prausnitz [17]:

$$\tau_{ij} = \frac{g_{ij} - g_{jj}}{RT} \tag{2}$$

In order to reduce the number of parameters correlated, the non-randomness parameter α of the NRTL model was set to 0.3. The remaining model parameters were adjusted to the VLE data using a flash-type objective function, as the largest uncertainty is associated with both the vapor and liquid phase compositions. The flash-type objective function is:

$$F = 100/N_p \left[\sum_1^{N_p} \left(\frac{x_{exp} - x_{cal}}{x_{exp}} \right)^2 + \sum_1^{N_p} \left(\frac{y_{exp} - y_{cal}}{y_{exp}} \right)^2 \right] \tag{3}$$

where N_p is the number of data points, x and y are the liquid and vapor phase compositions respectively, and the subscripts *exp* and *cal* denote the measured and calculated quantities. The objective function was minimized and the model parameters adjusted using the Levenberg-Marquardt algorithm [24]. We statistically analyze the quality of the data-fit using

the average absolute deviation (AAD), average absolute relative deviation (AARD) and the Bias. The AAD is:

$$AAD(\bar{\theta}) = \frac{1}{N_p}\sum_{1}^{N_p}\left|\bar{\theta}_{exp} - \bar{\theta}_{calc}\right| \tag{4}$$

where $\bar{\theta}_{exp}$ and $\bar{\theta}_{calc}$ are the experimental and calculated values of a measurand $\bar{\theta}$ (in this case x_1 and y_1), and N_p is the total number of data points. The AARD and Bias are defined as:

$$AARD(\bar{\theta}) = \frac{1}{N_p}\sum_{1}^{N_p}\frac{\left|\bar{\theta}_{exp} - \bar{\theta}_{calc}\right|}{\bar{\theta}_{exp}} \tag{5}$$

$$Bias(\bar{\theta}) = \frac{1}{N_p}\sum_{1}^{N_p}\frac{\bar{\theta}_{exp} - \bar{\theta}_{calc}}{\bar{\theta}_{exp}} \tag{6}$$

3. Results and discussion

Experimental vapor pressure data for R1270 are reported in table 3. The *P-T* data were modelled using the PR equation of state with the MC alpha function. The deviations of the data correlated by the model from experimental data are listed in table 3. The model accurately represents the vapor pressure data for R1270. The experimental vapor pressure data for R1270 were also compared to reference values from REFPROP [25], the resulting average absolute deviation for pressure is 0.33%.

P-x-y data are reported for the binary system of R1270 (1) + R1216 (2) at five temperatures, T = (288.07, 293.09, 299.47, 308.09 and 318.09) K in table 4. *P-x-y* data are reported for the binary system of R1270 (1) + HFPO (2) at five temperatures, T = (279.36, 288.19, 298.35, 308.18 and 317.12) K in table 5. Positive deviation from Raoult's law is observed for both binary systems, resulting in the formation of pressure-maximum azeotropes for all of the measured isotherms (figures 1 and 2). The previously measured *P-x-y* data of Coquelet *et al.* [6] for the binary system of R1270 (1) + R1216 (2) at 293.12 K are plotted and compared to our experimental data at 293.09 K in figure 1. The data agree with that of Coquelet *et al.* [6] to within the experimental uncertainties.

The model parameters and deviations between the experimental and modelled data using the PR equation of state coupled with the WS mixing rule and NRTL activity coefficient model are listed in table 6. The model parameters were fitted, firstly, individually to each isothermal data of each binary system, and secondly, simultaneously to data of all isotherms of each binary system respectively. The latter is more useful as it results in a single set of model parameters which can be used to describe all measured isotherms for a particular system in this study. The model parameters as well as the AAD, AARD and Bias are listed in table 6. The performance of the model is similar for both systems; an average AAD of approximately 0.003 for both the liquid and vapor phase compositions is achieved. For comparison, we

present *P-x-y* data predicted for the binary system of R1270 (1) + R1216 (2) using model parameters regressed from the data measured by Coquelet *et al.* [6]. Although, there is slight disagreement between the data, the data agrees to within the experimental uncertainty. The calculated azeotropic compositions and pressures for both binary systems are given in table 7. The azeotropic conditions agree well with those defined by Coquelet *et al.* [6]. Lastly, the relative volatility plots are displayed in figures 3 and 4 for the R1270 (1) + R1216 (2) and R1270 (1) + HFPO (2) binary systems respectively.

Conclusion

P-x-y data are reported for binary mixtures of propene with either 1,1,2,3,3,3-hexafluoroprop-1-ene or 2,2,3-trifluoro-3-(trifluoromethyl)oxirane at temperatures ranging from (279.36 to 318.09) K. The two binary systems exhibit a pressure-maximum azeotrope at all measured temperatures. The data are well correlated using a single set of binary interaction parameters across the entire temperature range for each system using the Peng-Robinson equation of state including the Mathias-Copeman alpha function, the Wong-Sandler mixing rule and the Non-Random Two Liquid activity coefficient model.

References

[1] C. Coquelet, D. Ramjugernath, H. Madani, A. Valtz, P. Naidoo, A.H. Meniai, J. Chem. Eng. Data 55 (2010) 2093-2099.
[2] M. Dicko, G. Belaribi-Boukais, C. Coquelet, A. Valtz, F.B. Belaribi, P. Naidoo, D. Ramjugernath, Ind. Eng. Chem. Res. 50 (2011) 4761-4768.
[3] E. El Ahmar, A. Valtz, P. Naidoo, C. Coquelet, D. Ramjugernath, J. Chem. Eng. Data 56 (2011) 1918-1924.
[4] A. Valtz, X. Courtial, E. Johansson, C. Coquelet, D. Ramjugernath, Fluid Phase Equilib. 304 (2010) 44-51.
[5] D. Ramjugernath, A. Valtz, C. Coquelet, D. Richon, J. Chem. Eng. Data 54 1292-1296.
[6] C. Coquelet, A. Valtz, P. Naidoo, D. Ramjugernath, D. Richon, J. Chem. Eng. Data 55 (2010) 1636-1639.
[7] S.C. Subramoney, A. Valtz, C. Coquelet, D. Richon, P. Naidoo, D. Ramjugernath, J. Chem. Thermodyn. 61 (2013) 18-26.
[8] W.M. Nelson, S.C. Subramoney, A. Valtz, C. Coquelet, D. Richon, P. Naidoo, D. Ramjugernath, J. Chem. Eng. Data. 56 (2011) 74-78.
[9] S.C. Subramoney, W.M. Nelson, A. Valtz, C. Coquelet, D. Richon, P. Naidoo, D. Ramjugernath, J. Chem. Eng. Data 55 (2010) 411-418.
[10] S.C. Subramoney, X. Courtial, P. Naidoo, C. Coquelet, D. Richon, D. Ramjugernath, Fluid Phase Equilib. 353 (2013) 7-14.
[11] S.C. Subramoney, A. Valtz, C. Coquelet, D. Richon, P. Naidoo, D. Ramjugernath, J. Chem. Eng. Data 57 (2012) 2947-2955.
[12] W.M. Nelson, M. Williams-Wynn, S.C. Subramoney, D. Ramjugernath, J. Chem. Eng. Data 60 (2015) 568-573.
[13] B. Holderbaum, J. Gmehling, Fluid Phase Equilib.70 (1991) 251-265.
[14] D.Y. Peng, D.B. Robinson, Ind. Eng. Chem. Fundam. 15 (1976) 59-64.
[15] P.M. Mathias, T.W. Copeman, Fluid Phase Equilib. 13 (1983) 91-108.
[16] D.S.H. Wong, S.I. Sandler, AIChE J. 38 (1992) 671-680.
[17] H. Renon, J.M. Prausnitz, AIChE J. 14 (1968) 135-144.
[18] M.M. Tshibangu, High pressure vapor-liquid equilibrium data of fluorochemical systems for various temperatures using a new static apparatus, M.Sc. Thesis, Chemical Engineering, University of KwaZulu-Natal, South Africa, 2010.
[19] S. Laugier, D. Richon, Rev. Sci. Instrum. 57 (1986) 469-472.
[20] A. Valtz, C. Coquelet, A. Baba-Ahmed, D. Richon, Fluid Phase Equilib. 202 (2002) 29-47.
[21] P. Guilbot, A. Valtz, H. Legendre, D. Richon, Analusis 28 (2000) 426-431.
[22] P.J. Mohr, B.N. Taylor, D.B. Newell, "The 2010 CODATA Recommended Values of the Fundamental Physical Constants" (Web Version 6.0), Available: http://physics.nist.gov/constants, National Institute of Standards and Technology, Gaithersburg, MD 20899, 2011.
[23] C. Coquelet, A. Baba-Ahmed, THERMOPACK version 1.10, 2005.
[24] D.W. Marquardt, J. Soc. Ind. Appl. Math. 11 (1963) 431-441.
[25] E.W. Lemmon, M.L. Huber, M.O. McLinden, Reference Fluid Thermodynamic and Transport Properties (REFPROP), NIST Standard Reference Database 23, Physical and Chemical Properties Division, National Institute of Standards and Technology, Gaithersburg, 2007.
[26] C. Coquelet, D. Ramjugernath, H. Madani, P. Naidoo, A.H. Meniai, J. Chem. Eng. Data 55 (2010) 2093 - 2099.

Acknowledgements

This work is based upon research supported by the National Research Foundation of South Africa under the South African Research Chair Initiative of the Department of Science and Technology.

TABLE 1

Pure-component parameters and properties for propene (R1270), hexafluoropropylene (R1216) and hexafluoropropylene oxide (HFPO).

	R1270 [6]	R1216 [26]	HFPO [2]
Component characterization			
CAS no.	115-07-1	116-15-4	428-59-1
Molecular formula	C_3H_6	C_3F_6	C_3F_6O
Supplier and purity	99.95 (Air Products)	99.9 (Pelchem)	99.9 (Pelchem)
GC Area	>99.95	>99.9	>99.9
Purification method	Degassed	Degassed	Degassed
Critical properties and acentric factor			
T_c (K)	364.9	358.9	359.3
P_c (MPa)	4.600	3.136	2.931
ω	0.1376	0.3529	0.3338
Matthias-Copeman (MC) coefficients			
c_1	0.6920[a]	0.8926	0.8749[b]
c_2	-2.105	-0.5100	-0.3222
c_3	11.253	3.1585	1.422

[a] MC parameters for R1270 regressed from our experimental vapor pressure data.
[b] MC parameters for HFPO regressed from vapor pressure data of Dicko *et al.* [2].

TABLE 1

Standard uncertainty estimates and influences for the variables (pressure (P), temperature (T) and the liquid (x) and vapour (y) phase compositions) of this work.

source of uncertainty	estimate[a]	distribution	influence
P from CPH 6000 /kPa	0.2	rectangular	P
correlation for P/kPa	8	rectangular	P
T from CTH 6500/K	0.02	rectangular	T
correlation for T/K	0.05	rectangular	T
correlation for n of R-1270[b]	1.5 %	rectangular	x, y
correlation for n of R-1216[b]	1.5 %	rectangular	x, y
correlation for n of HFPO[b]	2.0 %	rectangular	x, y
Volume of injected gas from syringe[c]	2 %	rectangular	x, y
T of injected gas from syringe[c] /K	2	rectangular	x, y
P of injected gas from syringe[c] /kPa	1	rectangular	x, y
repeatability (average) of x_i	$\bar{\sigma}_x = 0.002$	Gaussian	x
repeatability (average) of y_i	$\bar{\sigma}_y = 0.002$	Gaussian	y

[a] Estimate treated as either a type A or type B distribution

[b] Correlation of the number of moles (n) versus TCD peak area obtained by injecting known volumes of gas.

[c] Uncertainties inherent to the direct injection method, estimated from the ideal gas law.

TABLE 2

Experimental vapor pressure data for R1270, including a comparison of the data to REFPROP [25] and data fitted to the PR equation of state using the MC alpha function.

		REFPROP/MPa			PR-MC/MPa		
T_{exp}/K	P_{exp}/MPa	P_{cal}/MPa	ΔP/MPa[a]	$(\Delta P/P_{exp})$/%	P_{cal}/MPa	ΔP/MPa[a]	$(\Delta P/P_{exp})$/%
282.97	0.769	0.775	-0.006	-0.78	0.768	0.001	0.07
287.57	0.873	0.878	-0.005	-0.57	0.875	-0.002	-0.19
293.48	1.028	1.026	0.002	0.24	1.025	0.003	0.27
298.02	1.152	1.151	0.002	0.13	1.152	0.000	0.01
302.83	1.291	1.295	-0.004	-0.29	1.298	-0.007	-0.50
307.67	1.458	1.453	0.005	0.36	1.456	0.002	0.14
314.06	1.691	1.683	0.008	0.50	1.685	0.006	0.35
318.36	1.854	1.852	0.003	0.15	1.853	0.001	0.06
322.91	2.039	2.043	-0.004	-0.21	2.044	-0.004	-0.22
327.27	2.239	2.240	-0.002	-0.08	2.239	0.000	-0.02

[a] $\Delta P = P_{exp} - P_{cal}$, where P_{exp} and P_{cal} are the experimental and calculated vapor pressures respectively.
Expanded uncertainties (k = 2): $U(T)$ = 0.07 K; $U(P)$ = 0.008 MPa

TABLE 3

Experimental *P*-*x*-*y* data, including the temperature (*T*), pressure (*P*) and the liquid and vapour phase compositions (x_1 and y_1), for the binary system of R1270 (1) + R1216 (2) and the combined expanded uncertainty (*U*) (*k* = 2) for x_1 and y_1.

T/K	*P*/MPa	x_1	y_1	$U(x_1)$	$U(y_1)$
288.07	0.627	0.076	0.182	0.003	0.006
288.07	0.723	0.193	0.359	0.007	0.010
288.07	0.801	0.298	0.468	0.009	0.011
288.07	0.862	0.421	0.562	0.011	0.011
288.07	0.915	0.589	0.665	0.011	0.010
288.07	0.932	0.684	0.723	0.009	0.009
288.07	0.938	0.802	0.797	0.007	0.007
288.07	0.929	0.896	0.876	0.004	0.005
288.07	0.906	0.960	0.943	0.002	0.002
293.09	0.734	0.089	0.199	0.004	0.007
293.09	0.821	0.182	0.334	0.006	0.010
293.09	0.891	0.261	0.421	0.008	0.011
293.09	0.932	0.320	0.471	0.009	0.011
293.09	0.972	0.391	0.532	0.010	0.011
293.09	1.021	0.512	0.612	0.011	0.010
293.09	1.069	0.692	0.722	0.009	0.009
293.09	1.072	0.792	0.788	0.007	0.007
293.09	1.066	0.870	0.848	0.005	0.006
293.09	1.042	0.939	0.921	0.003	0.003
299.47	0.854	0.072	0.153	0.003	0.006
299.47	0.939	0.141	0.266	0.005	0.008
299.47	0.982	0.182	0.320	0.006	0.009
299.47	1.042	0.241	0.388	0.008	0.010
299.47	1.092	0.303	0.446	0.009	0.011
299.47	1.142	0.371	0.505	0.010	0.011
299.47	1.204	0.491	0.590	0.011	0.011
299.47	1.218	0.521	0.610	0.011	0.010
299.47	1.266	0.831	0.816	0.006	0.007

299.47	1.238	0.930	0.910	0.003	0.004
308.09	1.134	0.112	0.210	0.004	0.007
308.09	1.242	0.203	0.328	0.007	0.009
308.09	1.333	0.290	0.416	0.009	0.011
308.09	1.432	0.405	0.512	0.010	0.011
308.09	1.512	0.537	0.610	0.011	0.010
308.09	1.551	0.692	0.714	0.009	0.009
308.09	1.556	0.832	0.815	0.006	0.007
308.09	1.539	0.896	0.869	0.004	0.005
308.09	1.511	0.953	0.933	0.002	0.003
318.09	1.423	0.096	0.173	0.004	0.006
318.09	1.542	0.178	0.277	0.006	0.009
318.09	1.692	0.291	0.401	0.009	0.010
318.09	1.852	0.457	0.538	0.011	0.011
318.09	1.950	0.642	0.670	0.010	0.010
318.09	1.965	0.711	0.721	0.009	0.009
318.09	1.964	0.803	0.790	0.007	0.007
318.09	1.948	0.862	0.841	0.005	0.006
318.09	1.916	0.924	0.901	0.003	0.004

Expanded uncertainties (k = 2): $U(T)$ = 0.07 K; $U(P)$ = 0.008 MPa

TABLE 4

Experimental *P*-*x*-*y* data, including the temperature (*T*), pressure (*P*) and the liquid and vapour phase compositions (x_1 and y_1), for the binary system of R1270 (1) + HFPO (2) and the combined expanded uncertainty (*U*) (*k* = 2) for x_1 and y_1.

T/K	*P*/MPa	x_1	y_1	$U(x_1)$	$U(y_1)$
279.36	0.643	0.243	0.448	0.008	0.011
279.36	0.690	0.354	0.516	0.010	0.011
279.36	0.719	0.445	0.566	0.012	0.011
279.36	0.737	0.516	0.605	0.012	0.011
279.36	0.755	0.617	0.661	0.011	0.010
279.36	0.763	0.698	0.708	0.010	0.010
279.36	0.764	0.759	0.745	0.009	0.009
279.36	0.755	0.860	0.816	0.006	0.007
279.36	0.749	0.891	0.842	0.004	0.006
279.36	0.736	0.931	0.882	0.004	0.005
279.36	0.723	0.962	0.918	0.002	0.004
288.19	0.694	0.104	0.282	0.004	0.009
288.19	0.759	0.156	0.349	0.006	0.010
288.19	0.823	0.238	0.419	0.008	0.011
288.19	0.867	0.320	0.470	0.010	0.012
288.19	0.904	0.399	0.520	0.011	0.011
288.19	0.941	0.508	0.583	0.012	0.011
288.19	0.963	0.586	0.637	0.011	0.010
288.19	0.975	0.655	0.682	0.010	0.010
288.19	0.970	0.836	0.805	0.006	0.007
288.19	0.963	0.863	0.828	0.005	0.007
288.19	0.956	0.886	0.852	0.005	0.006
288.19	0.928	0.949	0.918	0.002	0.004
298.35	0.814	0.050	0.164	0.002	0.006
298.35	0.890	0.091	0.241	0.004	0.008
298.35	0.975	0.151	0.318	0.006	0.010
298.35	1.057	0.237	0.390	0.008	0.011
298.35	1.119	0.314	0.449	0.010	0.011

298.35	1.187	0.425	0.523	0.011	0.011
298.35	1.243	0.553	0.611	0.012	0.011
298.35	1.273	0.717	0.722	0.009	0.009
298.35	1.259	0.841	0.823	0.006	0.007
298.35	1.253	0.869	0.840	0.005	0.006
298.35	1.232	0.913	0.889	0.004	0.004
308.18	1.230	0.149	0.289	0.006	0.009
308.18	1.297	0.201	0.336	0.007	0.010
308.18	1.363	0.265	0.386	0.009	0.011
308.18	1.446	0.356	0.453	0.010	0.011
308.18	1.543	0.495	0.555	0.012	0.011
308.18	1.584	0.583	0.622	0.011	0.011
308.18	1.606	0.659	0.683	0.010	0.010
308.18	1.598	0.822	0.810	0.007	0.007
308.18	1.592	0.849	0.827	0.006	0.007
308.18	1.584	0.861	0.845	0.005	0.006
308.18	1.558	0.908	0.894	0.004	0.005
308.18	1.536	0.945	0.927	0.002	0.003
317.12	1.363	0.082	0.175	0.005	0.007
317.12	1.519	0.160	0.272	0.006	0.009
317.12	1.661	0.265	0.359	0.009	0.010
317.12	1.752	0.337	0.421	0.010	0.011
317.12	1.820	0.406	0.475	0.011	0.011
317.12	1.877	0.481	0.531	0.011	0.011
317.12	1.916	0.540	0.580	0.012	0.011
317.12	1.932	0.569	0.604	0.011	0.011
317.12	1.965	0.668	0.687	0.010	0.010
317.12	1.949	0.835	0.821	0.006	0.007
317.12	1.924	0.878	0.867	0.005	0.005
317.12	1.895	0.921	0.908	0.003	0.005

Expanded uncertainties ($k = 2$): $U(T) = 0.07$ K; $U(P) = 0.008$ MPa

TABLE 5

Model parameters regressed for the PR equation of state (MC alpha function) involving the WS mixing rule (k_{ij}) and NRTL activity coefficient model (τ_{ij}), and statistical analysis of the data-fit for the liquid and vapour phase compositions (x_1 and y_1).

	model parameters			**statistical analysis**					
Temperature/K	τ_{12}/J.mol^{-1}	τ_{21}/J.mol^{-1}	k_{12}	AAD(x_1)	AARD(x_1)/%	Bias(x_1)/%	AAD(y_1)	AARD(y_1)/%	Bias(y_1)/%
				R1270 (1) + R1216 (2)					
288.07	2522	697	0.120	0.003	1.44	-0.47	0.004	1.18	-0.48
293.09	2557	726	0.109	0.004	0.98	0.07	0.004	0.75	-0.10
299.47	2547	686	0.120	0.001	0.58	0.38	0.002	0.57	-0.47
308.09	2619	666	0.108	0.005	1.13	0.50	0.004	0.81	0.27
318.09	2701	303	0.138	0.002	0.71	0.15	0.002	0.41	0.13
(298.07 – 308.09)[a]	2634	678	0.112	0.004	1.25	0.47	0.005	1.05	0.11
				R1270 (1) + HFPO (2)					
279.36	5971	5073	-0.303	0.004	0.63	0.14	0.004	0.56	-0.28
288.19	5230	4888	-0.247	0.003	1.17	0.76	0.002	0.35	-0.14
298.35	5150	4489	-0.225	0.002	0.70	-0.37	0.003	0.48	0.48
308.18	5205	4248	-0.217	0.003	0.76	-0.68	0.003	0.39	0.39
317.12	4923	3971	-0.184	0.002	0.66	-0.52	0.003	0.48	0.37
(279.36 – 317.12)[a]	5406	4556	-0.244	0.004	0.93	-0.21	0.005	0.97	0.30

[a] Binary interaction parameters regressed over all isotherms simultaneously.

TABLE 6

Azeotropic pressures (P) and compositions (x_1) calculated via the PR equation of state coupled with the WS mixing rule and NRTL equation of state. Azeotropic conditions calculated from the correlations given by Coquelet *et al.* [6] for the binary system of R1270 (1) + R1216 (2) appear in the parentheses.

T/K	P/MPa	x_1
	R1270 (1) + R1216 (2)	
288.07	0.939 (0.939)	0.785 (0.787)
293.09	1.076 (1.074)	0.780 (0.781)
299.47	1.269 (1.267)	0.773 (0.775)
308.09	1.566 (1.566)	0.763 (0.765)
318.09	1.970 (1.973)	0.750 (0.754)
	R1270 (1) + HFPO (2)	
279.36	0.764	0.740
288.19	0.980	0.739
298.35	1.274	0.734
308.18	1.613	0.729
317.12	1.971	0.722

Expanded uncertainties (k = 2): $U(T)$ = 0.07 K; $U(P)$ = 0.008 MPa; $U(x)$ = 0.007

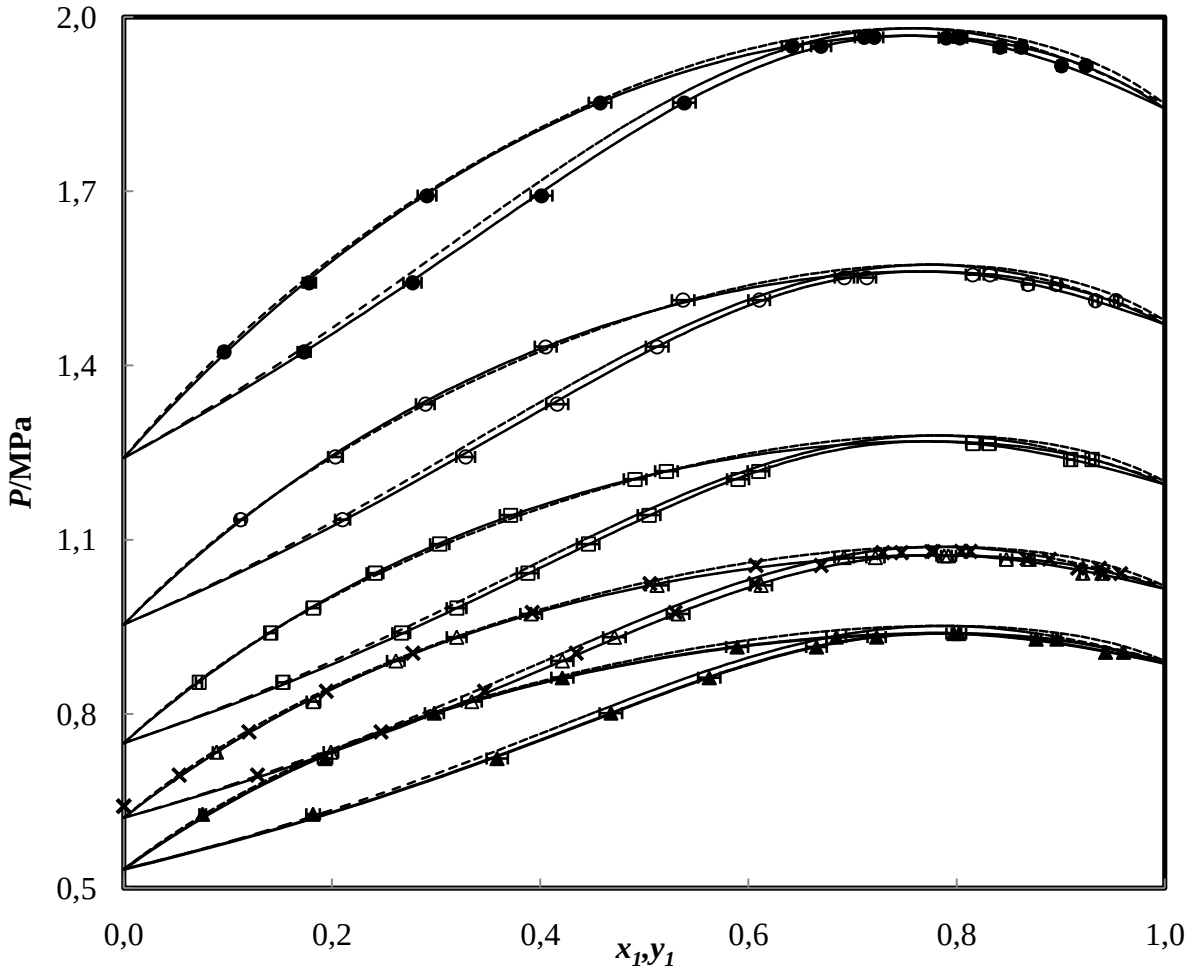

FIGURE 1. *P-x-y* data for the R1270 (1) + R1216 (2) binary system. Experimental data at: ▲ , 288.07 K; △, 293.09 K; □, 299.47 K; ○, 308.09 K; ●, 318.09 K; **×,** Coquelet *et al.* [6] at 293.12 K. Modelled data using the PR equation of state, MC alpha function, WS mixing rule and NRTL activity coefficient model: this work is represented by the solid black line; data predicted using the parameters of Coquelet *et al.* [6] are represented by the dashed line. Error bars indicate the expanded uncertainty (k = 2) for composition only.

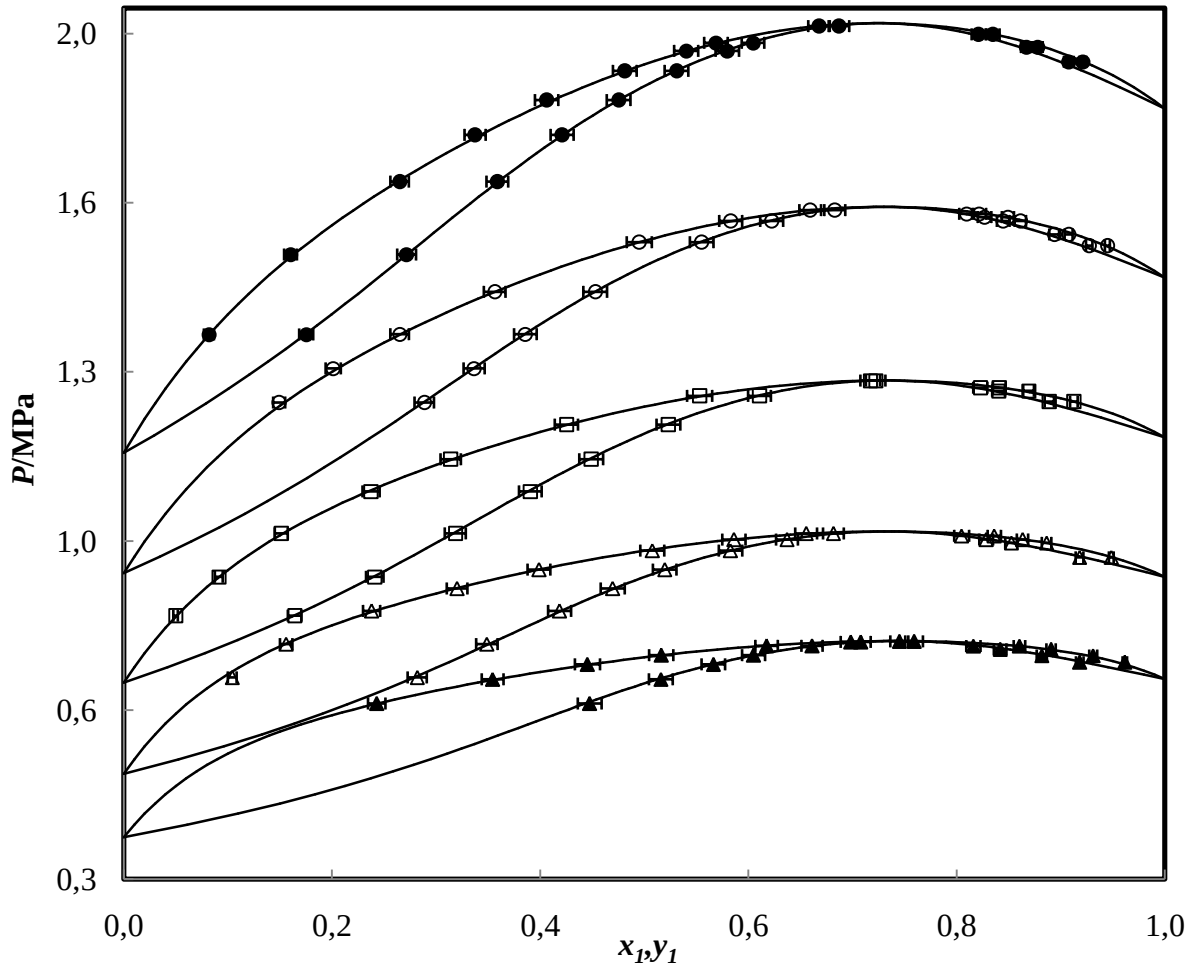

FIGURE 2. *P-x-y* data for the R1270 (1) + HFPO (2) binary system. Experimental data at: ▲, 279.36 K; △, 288.19 K ; □, 298.35 K; ○, 308.18 K; ●, 317.12 K. Modelled data using the PR equation of state, MC alpha function, WS mixing rule and NRTL activity coefficient model are represented by the solid black line. Error bars indicate the expanded uncertainty (*k* = 2) for composition only.

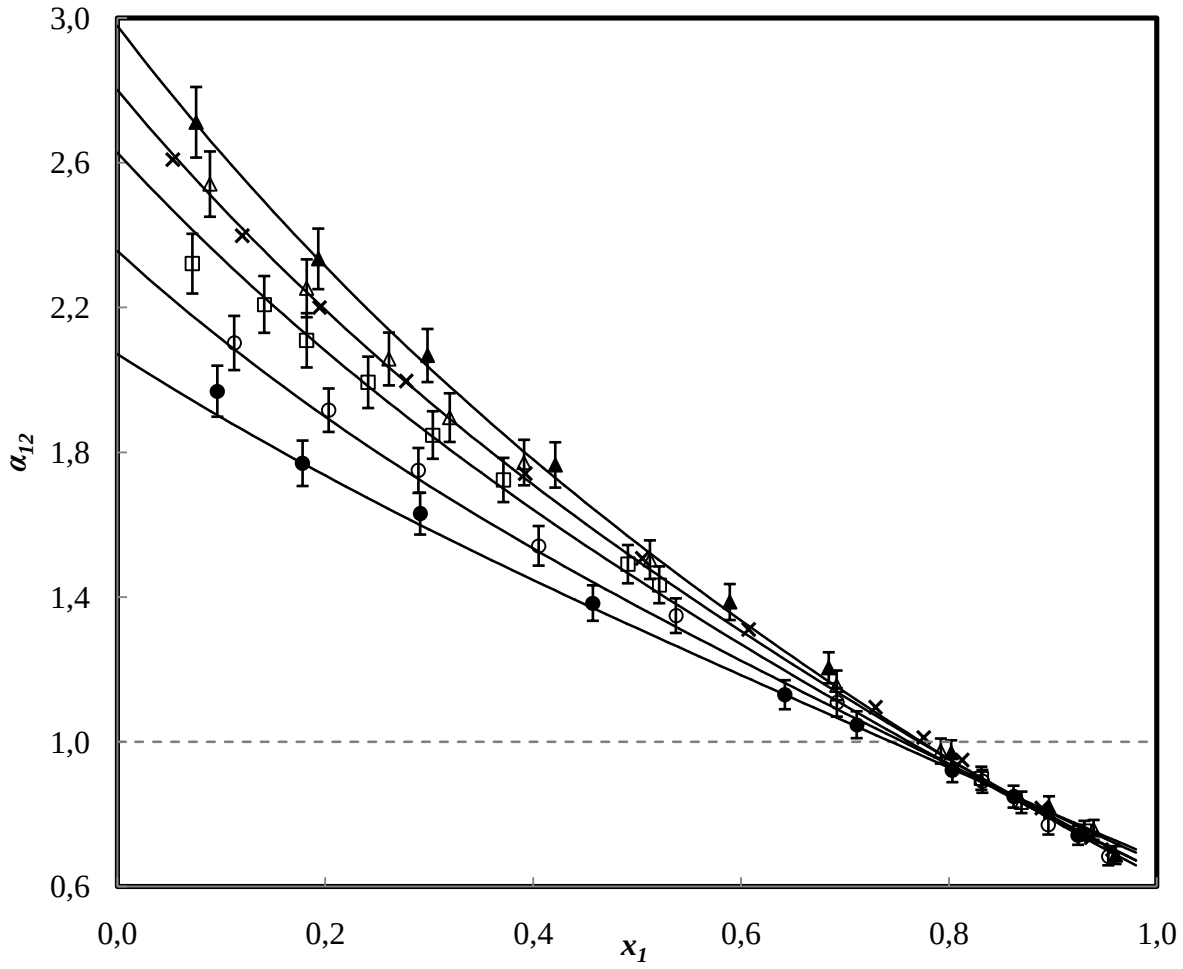

FIGURE 3. Plot of the relative volatility for the R1270 (1) + R1216 (2) binary system. Experimental data at: ▲, 288.07 K; △, 293.09 K; □, 299.47 K; ○, 308.09 K; ●, 318.09 K; ✕, Coquelet *et al.* [6] at 293.12 K. Modelled data using the PR equation of state, MC alpha function, WS mixing rule and NRTL activity coefficient model are represented by the solid black line. The dashed black line represents where the relative volatility is equal to unity. Error bars indicate the expanded uncertainty (k = 2) for the relative volatility only.

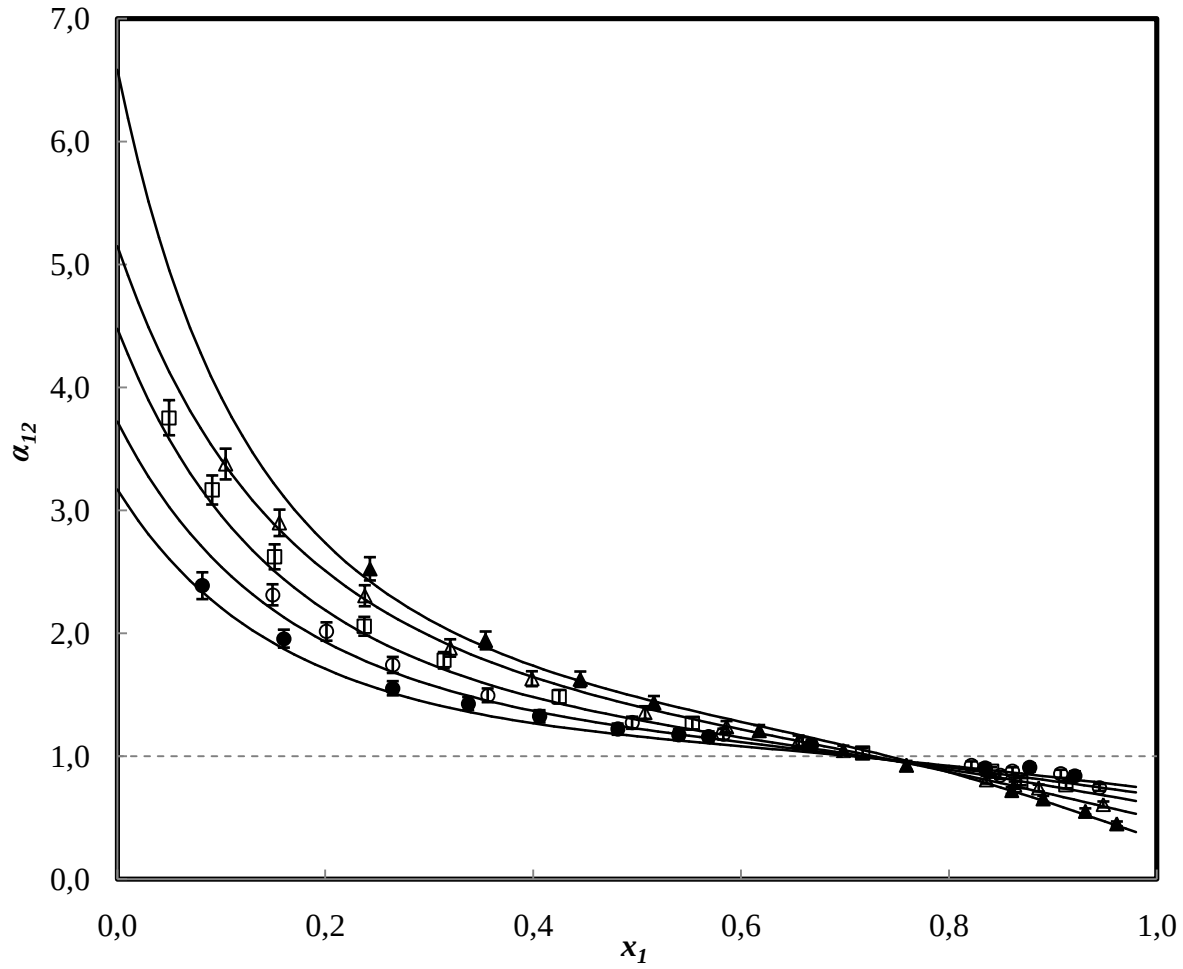

FIGURE 4. Plot of the relative volatility for the R1270 (1) + HFPO (2) binary system. Experimental data at: ▲, 279.36 K; △, 288.19 K ; □, 298.35 K; ○, 308.18 K; ●, 317.12 K. Modelled data using the PR equation of state, MC alpha function, WS mixing rule and NRTL activity coefficient model are represented by the solid black line. The dashed black line represents where the relative volatility is equal to unity. Error bars indicate the expanded uncertainty (k = 2) for the relative volatility only.